Measurement of the $Z \rightarrow \tau^+\tau^-$ production cross section in proton-proton collisions at 7 TeV center-of-mass energy with the ATLAS detector

D. Capriotti

Max-Planck-Institut für Physik
Werner Heisenberg Institut
Munich, 80805, Germany
capriott@mppmu.mpg.de

Introduction

Motivation for $Z \rightarrow \tau\tau$ analysis:

- cross section measurement of SM process, confirms the ATLAS measurement of $Z \rightarrow \mu\mu$ and $Z \rightarrow ee$,
- background for new particle searches in τ final states,
- unbiased source of τ-jets for calibration and efficiency measurements.

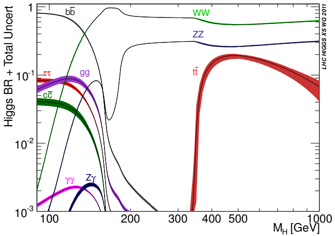

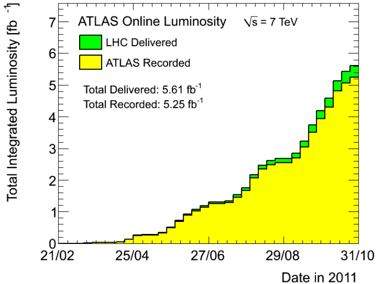

Part of 2011 data (integrated luminosity of 1.5 fb^{-1}) are used for the measurement in this thesis.

$Z \to \tau\tau$ final state

The final state depends on the decay modes of the τ leptons:

- τ leptonic decay: $\to l\nu_l\nu_\tau$ (35 %)
- τ hadronic decay: $\to had\ \nu_\tau$ (65 %)

Analysis of the semi-leptonic final state: 1 hadronic τ and 1 electron (muon).

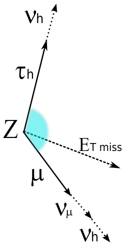

View of the $Z \to \tau\tau$ production in the transverse plane

- Isolated electron with high $p_T > 17$ GeV.
  or Isolated muon with high $p_T > 17$ GeV.
- Reconstructed and identified hadronic τ ($p_T > 20(25)$ GeV.
- Missing transverse energy due to the neutrinos' associated production.

Signal and Background

The reducible background is main due to the misidentification of hadronic τ decays by QCD jets, electrons and muons (low).

- Hadronic τ mainly composed of charged and neutral pions.
- Hadrons from τ decays are collimated along the τ direction.
- Low track multiplicity (1 or 3) corresponding to the charge pions produced.
- Algorithms developed to identify hadronic τs.

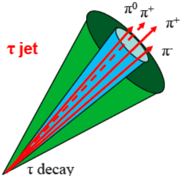

Signal and background processes:

$$\gamma^*/Z \to \ell\ell$$
$$\gamma^*/Z \to \ell\ell + \text{jet}$$
$$W \to \ell\nu + \text{jet}$$
$$W \to \tau\nu + \text{jet}$$
$$t\bar{t} \to W^+ b W^- \bar{b} \to \tau\nu\ell\nu + \text{jets}$$
Multijet

Signal and Background

The reducible background is main due to the misidentification of hadronic τ decays by QCD jets, electrons and muons (low).

- Hadronic τ mainly composed of charged and neutral pions.
- Hadrons from τ decays are collimated along the τ direction.
- Low track multiplicity (1 or 3) corresponding to the charge pions produced.
- Algorithms developed to identify hadronic τs.

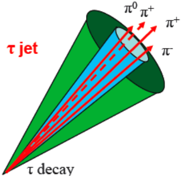

Signal and background processes:

$$\gamma^*/Z \to \ell\ell$$
$$\gamma^*/Z \to \ell\ell + \text{jet}$$
$$W \to \ell\nu + \text{jet}$$
$$W \to \tau\nu + \text{jet}$$
$$t\bar{t} \to W^+bW^-\bar{b} \to \tau\nu\ell\nu + \text{jets}$$
Multijet

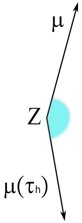

Signal and Background

The reducible background is main due to the misidentification of hadronic τ decays by QCD jets, electrons and muons (low).

- Hadronic τ mainly composed of charged and neutral pions.
- Hadrons from τ decays are collimated along the τ direction.
- Low track multiplicity (1 or 3) corresponding to the charge pions produced.
- Algorithms developed to identify hadronic τs.

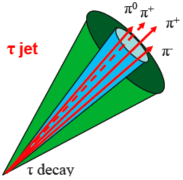

Signal and background processes:

$$\gamma^*/Z \to \ell\ell$$
$$\gamma^*/Z \to \ell\ell + \text{jet}$$
$$W \to \ell\nu + \text{jet}$$
$$W \to \tau\nu + \text{jet}$$
$$t\bar{t} \to W^+bW^-\bar{b} \to \tau\nu\ell\nu + \text{jets}$$
Multijet

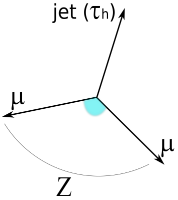

Signal and Background

The reducible background is main due to the misidentification of hadronic τ decays by QCD jets, electrons and muons (low).

- Hadronic τ mainly composed of charged and neutral pions.
- Hadrons from τ decays are collimated along the τ direction.
- Low track multiplicity (1 or 3) corresponding to the charge pions produced.
- Algorithms developed to identify hadronic τs.

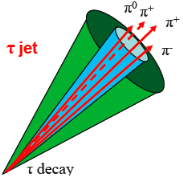

Signal and background processes:

$$\gamma^*/Z \to \ell\ell$$
$$\gamma^*/Z \to \ell\ell + \text{jet}$$
$$W \to \ell\nu + \text{jet}$$
$$W \to \tau\nu + \text{jet}$$
$$t\bar{t} \to W^+bW^-\bar{b} \to \tau\nu\ell\nu + \text{jets}$$
Multijet

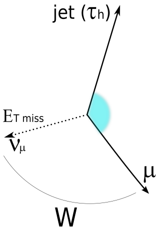

Signal and Background

The reducible background is main due to the misidentification of hadronic τ decays by QCD jets, electrons and muons (low).

- Hadronic τ mainly composed of charged and neutral pions.
- Hadrons from τ decays are collimated along the τ direction.
- Low track multiplicity (1 or 3) corresponding to the charge pions produced.
- Algorithms developed to identify hadronic τs.

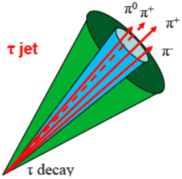

Signal and background processes:

$$\gamma^*/Z \rightarrow \ell\ell$$
$$\gamma^*/Z \rightarrow \ell\ell + \text{jet}$$
$$W \rightarrow \ell\nu + \text{jet}$$
$$W \rightarrow \tau\nu + \text{jet}$$
$$t\bar{t} \rightarrow W^+bW^-\bar{b} \rightarrow \tau\nu\ell\nu + \text{jets}$$
Multijet

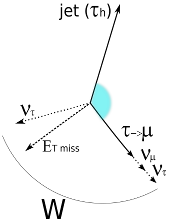

Signal and Background

The reducible background is main due to the misidentification of hadronic τ decays by QCD jets, electrons and muons (low).

- Hadronic τ mainly composed of charged and neutral pions.
- Hadrons from τ decays are collimated along the τ direction.
- Low track multiplicity (1 or 3) corresponding to the charge pions produced.
- Algorithms developed to identify hadronic τs.

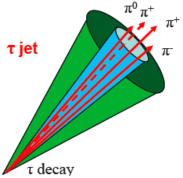

Signal and background processes:

$$\gamma^*/Z \to \ell\ell$$
$$\gamma^*/Z \to \ell\ell + \text{jet}$$
$$W \to \ell\nu + \text{jet}$$
$$W \to \tau\nu + \text{jet}$$
$$t\bar{t} \to W^+ bW^- \bar{b} \to \tau\nu\ell\nu + \text{jets}$$
Multijet

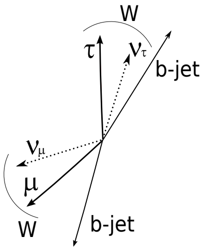

Signal and Background

The reducible background is main due to the misidentification of hadronic τ decays by QCD jets, electrons and muons (low).

- Hadronic τ mainly composed of charged and neutral pions.
- Hadrons from τ decays are collimated along the τ direction.
- Low track multiplicity (1 or 3) corresponding to the charge pions produced.
- Algorithms developed to identify hadronic τs.

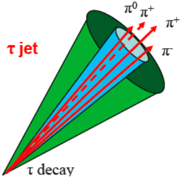

Signal and background processes:

$$\gamma^*/Z \to \ell\ell$$
$$\gamma^*/Z \to \ell\ell + \text{jet}$$
$$W \to \ell\nu + \text{jet}$$
$$W \to \tau\nu + \text{jet}$$
$$t\bar{t} \to W^+ b W^- \bar{b} \to \tau\nu\ell\nu + \text{jets}$$
Multijet

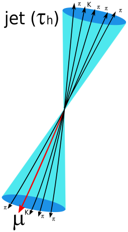

$Z \to \tau\tau$ selection

- Electroweak processes and $t\bar{t}$ are estimated by the Monte Carlo simulation, multi-jet background estimated from data.

✓ Events are selected with different triggers:

Trigger
- $\tau_\mu\tau_\mathrm{h}$ channel: muon with $\mathrm{p_T} > 15$ GeV plus isolation cuts
- $\tau_e\tau_\mathrm{h}$ channel: electron with $\mathrm{p_T} > 15$ GeV and τ with $\mathrm{p_T} > 16$ GeV

✓ Object selection

	Electrons	Muons	Hadronic τs
$\mathrm{p_T}$ min (GeV)	17	17	$20(\tau_\mu\tau_\mathrm{h}$ chan), $25(\tau_e\tau_\mathrm{h}$ chan)
	Identification and quality cuts		

✓ Isolation cuts on selected leptons to reduce the Multijet background.

Muon isolation

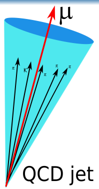

- Multi-jet QCD background gives the dominant contribution.
- Muons and electrons from $Z \to \tau\tau$ events are isolated, in contrast to those arising from jets.
- The isolation of muons is measured from the energy deposits and tracks momenta in an isolation cone of radius ΔR around the muon trajectory.

Track isolation

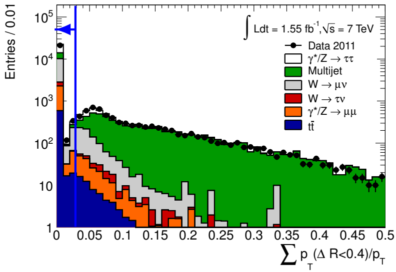

Calorimeter isolation

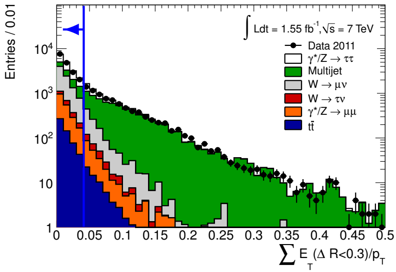

- Isolation cuts: $\sum p_T^{ID}/p_T^{\mu} < 0.03$ in $\Delta R = 0.40$ and $\sum E_T^{ID}/p_T^{\mu} < 0.04$ in $\Delta R = 0.30$

Event selection

- Events are selected with 1 isolated lepton and 1 selected hadronic τ whose charge is opposite.
- Electroweak and $t\bar{t}$ are estimated from Monte Carlo simulation: the number of W/Z +jet events are normalized to data with scaling factors (slide 9).
- The contribution of the multi-jet background is estimated from data (slide 10).

1) Di-lepton veto (see backup): events with > 1 preselected lepton are removed (against $t\bar{t}$, $Z \to \ell\ell$ and di-leptonic $Z \to \tau\tau$ decays).

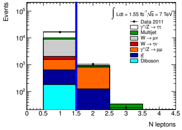

2) W suppression cuts (see backup): cut on the kinematic of the final state particles.

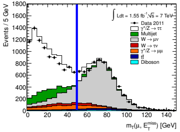

3) Hadronic τ cleaning (see backup): Cut on the numbers of tracks (1 or 3), electromagnetic fraction ($\tau_\mu \tau_\mathrm{h}$ only) and charge of the τ candidate.

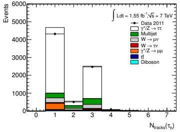

Event selection: Visible Mass

4) Visible Mass: The invariant mass between the lepton and the hadronic τ is $35 < M_{\text{vis}} < 75$ GeV.

$\tau_\mu \tau_\mathrm{h}$ channel

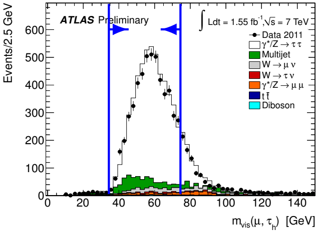

Data 2011	5184(72)
$Z/\gamma^* \to \tau\tau$	4544(49)
$W \to \mu\nu$	186(13)
$W \to \tau\nu$	49(5)
$Z/\gamma^* \to \mu\mu$	81(7)
$t\bar{t}$	31(1)
Diboson	15(2)
Multi-jet	432(30)

$\tau_e \tau_\mathrm{h}$ channel

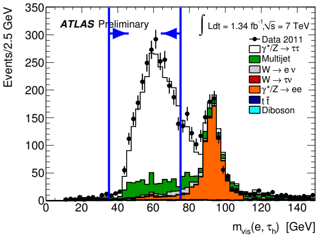

Data 2011	2600(51)
$Z/\gamma^* \to \tau\tau$	2029(25)
$W \to e\nu$	45(5)
$W \to \tau\nu$	18(2)
$Z/\gamma^* \to ee$	64(4)
$t\bar{t}$	17(1)
Dibosons	6(1)
Multi-jets	300(21)

Normalization of the W/Z + jet background to data

- Data and simulation compared in background enriched control regions.
- The number of W/Z simulated events is overestimated, after the τ identification cuts on the hadronic τ candidates.
- The number of simulated events is normalized to the number of events in data.

W control region: pass the dilepton veto and τ cleaning but fails both W suppression cuts.

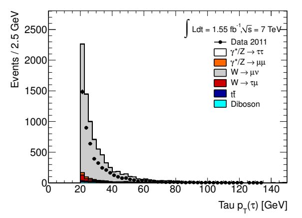

Normalization factors:

$$k_W = \begin{cases} 0.44 \pm 0.02 \text{ (stat.)} & \tau_e\tau_h \text{ channel} \\ 0.54 \pm 0.01 \text{ (stat.)} & \tau_\mu\tau_h \text{ channel} \end{cases}$$

Z control region: two electrons (muons) with an invariant mass close to the Z mass.

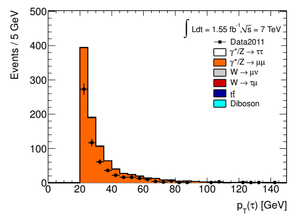

Normalization factors:

$$k_Z = \begin{cases} 0.39 \pm 0.05 \text{ (stat.)} & \tau_e\tau_h \text{ channel} \\ 0.57 \pm 0.04 \text{ (stat.)} & \tau_\mu\tau_h \text{ channel} \end{cases}$$

Estimation of the multijet background

- Data-driven technique for the multijet estimation
- Background-enriched control regions (B, C, D regions) defined by the inversion of the opposite sign and lepton isolation requirements

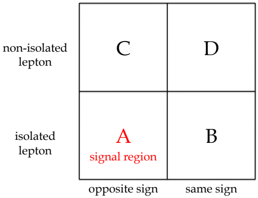

- The number of multi-jet events in the signal region is calculated from the ratio of multi-jet events in region C and D:

$$N^A_{\mathrm{Multi-jet}} = \frac{N^C_{\mathrm{Multi-jet}}}{N^D_{\mathrm{Multi-jet}}} N^B_{\mathrm{Multi-jet}} = R_{\mathrm{OSSS}} N^B_{\mathrm{Multi-jet}}$$

$$R_{\mathrm{OSSS}} = \begin{cases} 1.06 \pm 0.03\ (\text{stat.}) \pm 0.02\ (\text{iso sys.}) \pm 0.04\ (\text{cutflow sys.}) & \tau_e \tau_h \text{ channel}, \\ 1.13 \pm 0.04\ (\text{stat.}) \pm 0.02\ (\text{iso sys.}) & \tau_\mu \tau_h \text{ channel}. \end{cases}$$

The $Z \to \tau\tau$ cross section

$$\sigma(Z \to \tau\tau) \times BR(\tau \to l\nu\nu) \times BR(\tau \to \tau_{\text{had}}\nu) = \frac{N_{\text{obs}} - N_{\text{bkg}}}{A_Z \cdot C_Z \cdot \mathcal{L}}$$

$$2 \times \text{BR}(\tau \to \mu\,\nu\,\nu) \times \text{BR}(\tau \to \tau_{had}\,\nu) = 0.2250 \pm 0.0009,$$

$$2 \times \text{BR}(\tau \to e\,\nu\,\nu) \times \text{BR}(\tau \to \tau_{had}\,\nu) = 0.2313 \pm 0.0009.$$

	$\tau_\mu\tau_\text{h}$	$\tau_e\tau_\text{h}$
N_{obs} number of data events	5184 ± 72(stat.)	2600 ± 51(stat.)
N_{bkg} number of background events	793 ± 34(stat.)	449 ± 22(stat.)
A_Z acceptance	0.0976 ± 0.0002(stat.)	0.0687 ± 0.0002(stat.)
C_Z signal efficiency	0.1417 ± 0.0016(stat.)	0.1009 ± 0.0013(stat.)
$\mathcal{L}$ integrated luminosity	$1547.1\ \text{pb}^{-1}$	$1343.7\ \text{pb}^{-1}$

Muon channel

$$\sigma(Z \to \tau\tau, m_{inv} = 66 - 116\ GeV) = 0.91 \pm 0.02(\text{stat}) \pm 0.09(\text{syst}) \pm 0.03(\text{lumi})\ \text{nb}$$

Electron channel

$$\sigma(Z \to \tau\tau, m_{inv} = 66 - 116\ GeV) = 1.00 \pm 0.03(\text{stat}) \pm 0.14(\text{syst}) \pm 0.04(\text{lumi})\ \text{nb}$$

Conclusion

- Full analysis with 2011 data performed: good agreement between data and simulation means good understanding of detector performance in the reconstruction and identification of electrons, muons and hadronic τ leptons.
- Cross section measurement in the semi-leptonic channels is calculated with systematic uncertainties.
- Results from the semileptonic final state are combined with the dileptonic final state, the result of the combination is compatible with the theoretical prediction and the ATLAS measurements of Z$\rightarrow \mu\mu$ and Z$\rightarrow ee$ decays.

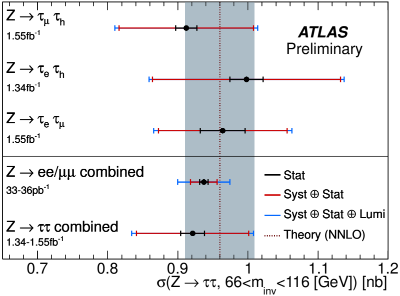

The $H \to \tau\tau$ analysis in ATLAS

- Analysis of $\tau_\ell\tau_\ell$, $\tau_h\tau_\ell$ and $\tau_h\tau_h$ final states (+jets).
- Production modes: gluon-gluon fusion ($gg \to H$), vector boson fusion ($qq \to qqH$) and Higgstrahlung ($q\bar{q} \to W(Z)H$) $\Rightarrow$ different categories depending on the number of jets
- $Z \to \tau\tau$ dominant background estimated with a $Z \to \tau\tau$ embedded technique from $Z \to \mu\mu$ events.

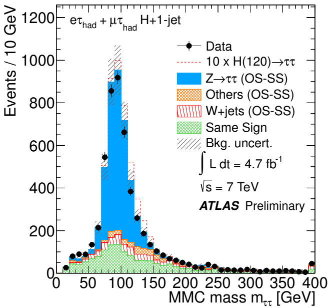

$H \to \tau\tau$ invariant mass ($\tau_\ell\tau_h$ + 1 jet)

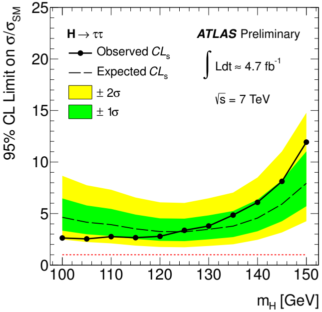

$H \to \tau\tau$ (all categories) exclusion plot

The $Z \to \tau\tau$ analysis in CMS with 36 pb^{-1}

- Analysis of $\tau_e\tau_\mu$, $\tau_\mu\tau_\mu$, $\tau_e\tau_h$ and $\tau_\mu\tau_h$ final states.
- Similar strategy but different τ identification (particle flow algorithm).
- Background estimation:
  - $\rightarrow$ multi-jet from SS to OS extrapolation with the ABCD method,
  - $\rightarrow$ W + jet from inversion of W suppression cuts
- Cross section compatible with ATLAS and theoretical predictions: signal shape and normalization from fit.

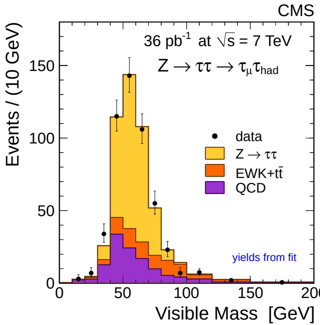

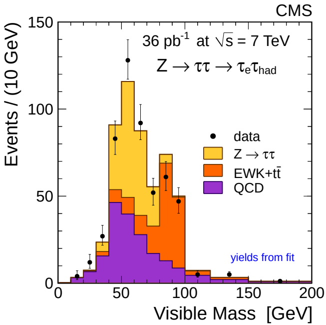

Reconstruction of hadronic τ leptons

The reconstruction of tau leptons is understood as a reconstruction of the hadronic τ-decay modes.
The definition of hadronic τ candidate is performed in two steps: reconstruction and identification.

- Hadronic τ candidates are reconstructed from calorimeter jets reconstructed with an anti-Kt algorithm within a cone of $\Delta R = 0.4$.
- Inner Detector tracks are associated to the calorimeter clusters if the distance from the axis of the seed jet is less than 0.2.
- Energy calculated from the deposits in the cells and calibrated.
- Discriminating variables are calculated.

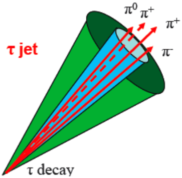

Three different discriminants are defined: simple cut-based selection, projective likelihood identification and identification with boosted decision tree (BDT).

The identification of reconstructed τ candidates is performed separately for 1-prong and multi-prong candidates.

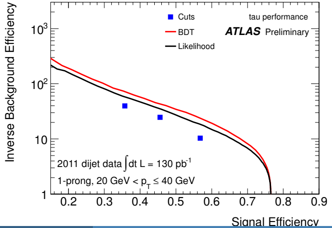

Reconstruction of muons

- ⇒ ID track: track reconstructed in the Inner Detector. High efficiency and good momentum resolution.
- ⇒ MS track: track reconstructed in the Muon Spectrometer. High muon purity: only muons reach the spectrometer.

Different algorithms are developed depending on the combination of ID and MS:

- ⇒ combined muon: successful combination of the ID and MS tracks,
- ⇒ segment-tagged muon: combination of the ID track with MS segments,

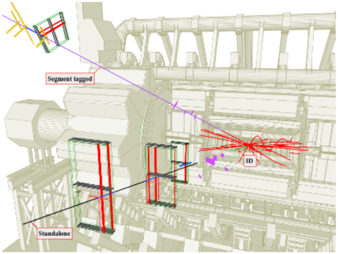

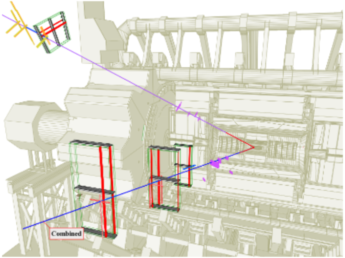

The $Z \to \mu\mu$ tag-and-probe method

Muons of the $Z \to \tau\tau$ analysis are reconstructed as segment-tagged or combined, isolated and triggered the event.
The relative efficiencies are measured with the tag-and-probe method.

- The method:

$\to$ select a clean sample of $Z \to \mu\mu$ events from data,

$\to$ tight requirement on one muon (tag) and loose criteria on the second muon (probe),

$\to$ efficiency of muons measured with respect to the probe.

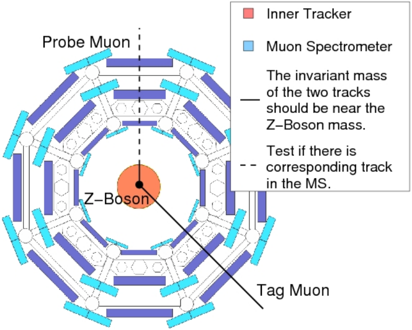

Measurement of the muon efficiencies

Muon reconstruction efficiency

$\epsilon = \epsilon_{ID}\ \epsilon_{MS}\ \epsilon_{\text{comb}}$

ϵ_{ID}

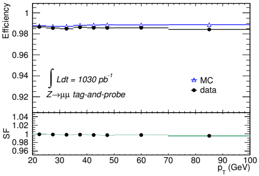

$\epsilon_{MS}\ \epsilon_{\text{comb}}$

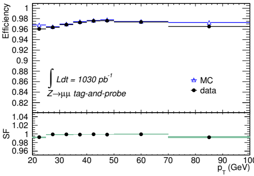

Muon isolation efficiency:
number of reconstructed muons that satisfy the isolation cuts.

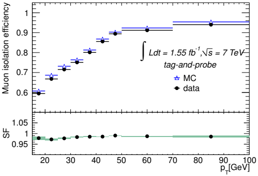

Muon trigger efficiency:
number of reconstructed and isolated muons that fired the trigger.

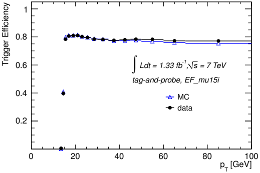

Measurement of the muon reconstruction efficiency (1)

Muon reconstruction efficiency $\epsilon = \epsilon_{ID}\ \epsilon_{MS}\ \epsilon_{\mathrm{comb}}$

- ID track efficiency ϵ_{ID} measured with respect to MS muons.

Efficiency as a function of $\mathrm{p_T}$

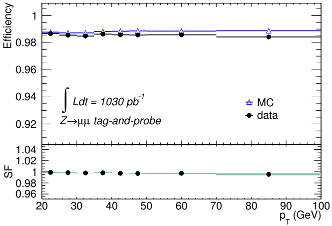

Efficiency as a function of the η

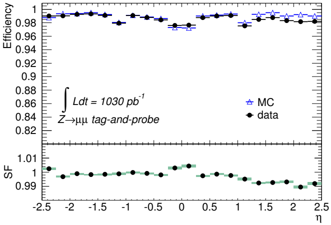

- Efficiency losses due to the Inner Detector hit requirements of the track.
- The integrated efficiency measured from collision data $(98.58 \pm 0.01)\%$ is slightly different from the efficiency measured by the Monte Carlo simulation $(98.81 \pm 0.01)\%$, in particular at $\eta > 1$ due to problem in one sector.

Measurement of the muon reconstruction efficiency (2)

- Combined efficiency $\epsilon_{MS}\ \epsilon_{\text{comb}}$ measured with respect to ID muons.

Efficiency as a function of p_T

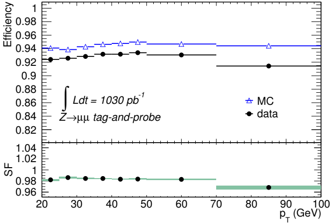

Efficiency as a function of the η

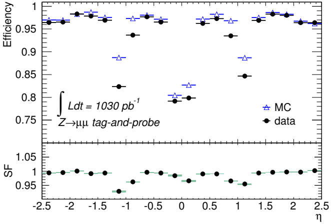

- Loss in efficiency: crack region at $\eta \sim 0$ and Barrel-Endcap overlap region (missing chambers). No MS track.
- Difference between data and simulation (perfect alignment).
- The efficiency measured from data is $(93.04 \pm 0.03)\%$, while the efficiency measured from Monte Carlo simulation is $(94.52 \pm 0.01)\%$.

Measurement of the muon reconstruction efficiency (3)

Efficiency can be recovered by including segment-tagged muons. Recover muons which did not cross enough precision chambers (Barrel-Endcap overlap).

- Segment-tagged plus combined muon efficiency with respect to ID muons.

Efficiency as a function of p_T

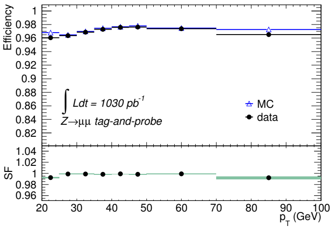

Efficiency as a function of the η

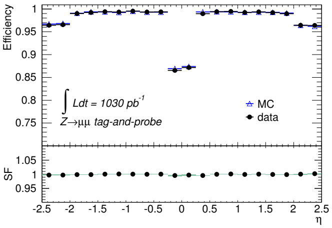

- The reconstruction efficiency measured in data is $(97.20 \pm 0.02)\%$, in good agreement with the efficiency measured from the Monte Carlo simulation $(97.30 \pm 0.01)\%$.

Measurement of the muon trigger efficiency

- Single muon trigger with p_T threshold at 15 GeV used for the $Z \rightarrow \tau\tau$ analysis. Event rate reduced by isolation cuts applied.

The muon trigger efficiency is calculated with respect to reconstructed and isolated muons.

Muon trigger efficiency

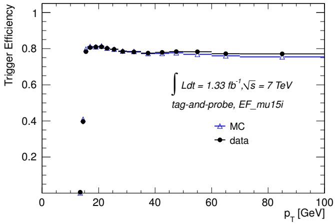

Efficiency in data periods

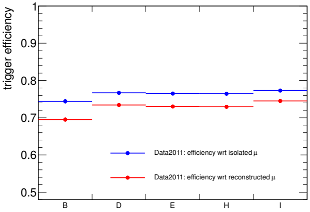

- The efficiency measured in data $(78.19 \pm 0.05)\%$ is slightly different to the one measured in the simulation $(75.89 \pm 0.15)\%$. Small correction applied to the Monte Carlo prediction (~ 0.02).
- Small dependence on the data periods.

Event selection

- Events are selected with 1 isolated lepton and 1 selected hadronic τ whose charge is opposite.
- Electroweak and $t\bar{t}$ are estimated from Monte Carlo simulation: the number of W/Z +jet events are normalized to data with scaling factors (slides 9, ??).
- The contribution of the multi-jet background is estimated from data (slide 10).

1) Di-lepton veto: events with > 1 preselected lepton are removed (against $t\bar{t}$, $Z \to \ell\ell$ and di-leptonic $Z \to \tau\tau$ decays).

$\tau_\mu \tau_\mathrm{h}$ channel

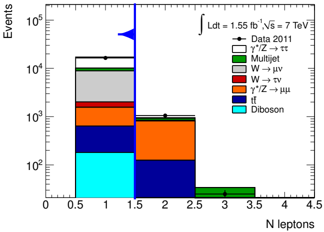

$\tau_e \tau_\mathrm{h}$ channel

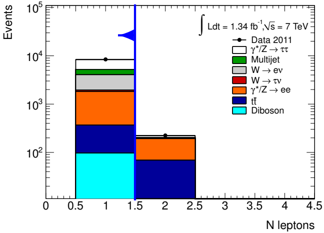

Event selection: W suppression cuts

2) W suppression cuts

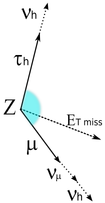

- τ leptons from Z decays are boosted: decay products are collimated along the τ direction.
- if Z bosons are boosted in the transverse plane, the E_T^{miss} vector falls in the angle between the decay products of the Z.

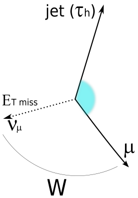

- In $W \to \ell\nu$ + jet events, neutrino, muon and jets point in different directions to balance the $\mathrm{p_T}$ of the W.
- The E_T^{miss} originates from the neutrino's energy and its trajectory is not in the angle between the lepton and the fake hadronic τ.

Two variables are defined:

$$\sum \cos\Delta\phi = \cos\left(\phi(\ell) - \phi(E_T^{\mathrm{miss}})\right) + \cos\left(\phi(\tau_\mathrm{h}) - \phi(E_T^{\mathrm{miss}})\right) \tag{1}$$

and

$$m_\mathrm{T}(\ell, E_T^{\mathrm{miss}}) = \sqrt{2\, p_\mathrm{T}(\ell) \cdot E_T^{\mathrm{miss}} \cdot (1 - \cos\Delta\phi(\ell, E_T^{\mathrm{miss}}))}\;. \tag{2}$$

Event selection: W suppression cuts (2)

2) W suppression cuts: $\sum \cos\Delta\phi >$ -0.15, $m_{\mathrm{T}}(\ell, E_T^{\mathrm{miss}}) < 50$ GeV

$\tau_\mu \tau_{\mathrm{h}}$ channel

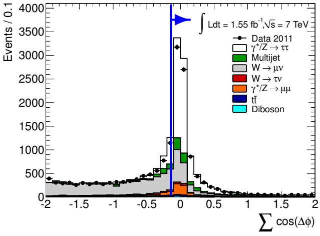

$\tau_e \tau_{\mathrm{h}}$ channel

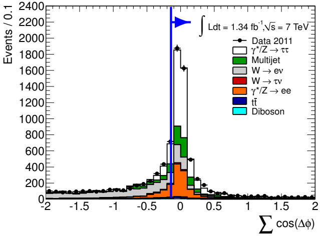

$\tau_\mu \tau_{\mathrm{h}}$ channel

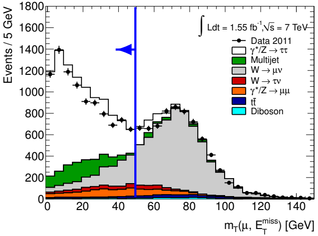

$\tau_e \tau_{\mathrm{h}}$ channel

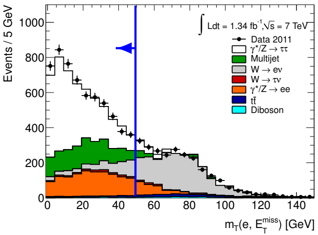

Event selection: hadronic τ cleaning

3) Hadronic τ cleaning: Cut on the numbers of tracks, electromagnetic fraction ($\tau_\mu \tau_h$ only) and charge of the τ candidate.

$\tau_\mu \tau_h$ channel

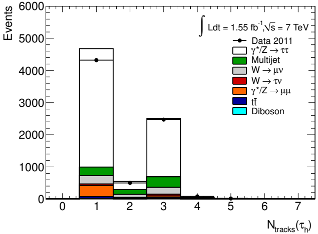

$\tau_e \tau_h$ channel

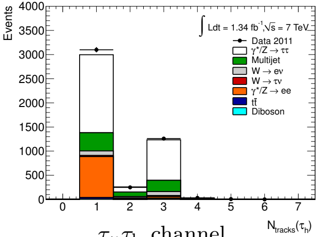

$\tau_\mu \tau_h$ channel

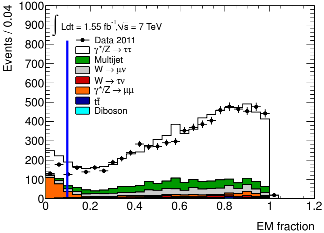

- The number of track of the τ candidate = 1 - 3 (jets have higher multiplicity).
- The electromagnetic fraction - energy in EM calorimeter over total calorimetric energy - is > 0.10. Details in the backup (slide 28).

Analysis of the $\mu \to \tau$ misidentification rate

- Excess of events is found at low values in the distribution of the electromagnetic fraction in the $\tau_\mu \tau_\mathrm{h}$ channel

$\Rightarrow$ excess in the $Z \to \mu\mu(\tau_\mathrm{h})$ contribution

Selection of a $Z \to \mu\mu$ enriched control region

τ number of tracks

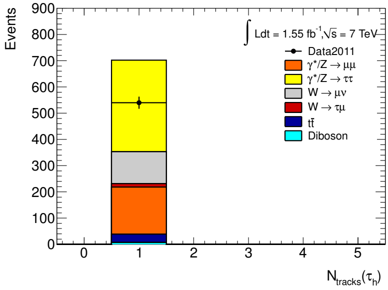

τ EM energy fraction

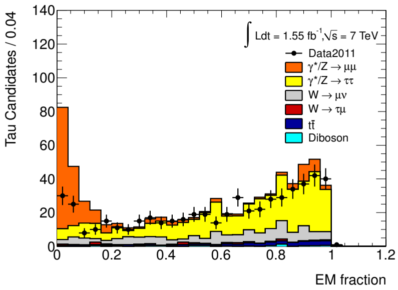

Systematic uncertainty

Main contributions:

- lepton SF: reconstruction-isolation-trigger scale factors are scaled upwards and downwards of 1σ at the same time.
- τ id efficiency: systematic error applied to identified τ candidates.
- e, τ and E_T^{miss} energy scale: main contribution due to the τ energy scale ($\sim 6\%$).

Systematic uncertainty	$\delta\sigma/\sigma$ (%) $\tau_\mu\tau_\text{h}$	$\delta\sigma/\sigma$ (%) $\tau_e\tau_\text{h}$
lepton SF	1.7	5.0
muon resolution	< 0.05	-
electron resolution	-	0.1
τ id efficiency	5.2	5.2
electron-tau jet rate	-	0.2
e, τ and E_T^{miss} energy scale	8.2	9.3
tau trigger	-	4.7
k_W	<0.05	<0.05
k_Z	<0.05	<0.05
Multi-jet estimation	0.8	1.3
MC cross sections	0.1	0.2
A_Z uncertainties	3.1	3.4
Total systematic unc.	10.4	13.2

Geometric and kinematic signal acceptance

- Extrapolate from the fiducial region (see Table) to the phase space

	$\tau_\mu \tau_\mathrm{h}$ channel	$\tau_e \tau_\mathrm{h}$ channel
Lepton	$\mathrm{p_T} > 17$ GeV	$E_T > 17$ GeV, $\lvert\eta\rvert < 2.47$
Lepton	$\lvert\eta\rvert < 2.4$	$\lvert\eta\rvert < 2.47$, excluding $1.37 < \lvert\eta\rvert < 1.52$
Tau	$E_T > 20$ GeV	$E_T > 25$ GeV, $\lvert\eta\rvert < 2.47$
Tau	$\lvert\eta\rvert < 2.47$, excluding $1.37 < \lvert\eta\rvert < 1.52$	$\lvert\eta\rvert < 2.47$, excluding $1.37 < \lvert\eta\rvert < 1.52$
Event	$\Sigma \cos \Delta\phi > -0.15$, $m_T < 50$ GeV, M_vis within [35, 75] GeV	

- Acceptance :

$$A_Z = \frac{N_\mathrm{fiducial}}{N_\mathrm{generated}}$$

- $N_\mathrm{generated}$ in $m_{\tau\tau}$ [66-116] GeV to reduce off-shell Z production.
- Photon radiation by τ leptons and their decay products is taken into account.

Combination of the results

- Cross section measurements are often correlated when they are performed by the same experiment
- Best Linear Unbiased Estimation (BLUE) method used, takes into account the uncertainty correlations.
- 3 measurements x_i corresponding to the $\tau_e\tau_\mu$, $\tau_\mu\tau_{\mathrm{h}}$ and $\tau_e\tau_{\mathrm{h}}$
- Linear combination:

  $$y = w_1x_1 + w_2x_2 + w_3x_3$$

  find the best weights w_i that minimize the variance

  $$Var(y) = \sum_i \sum_j w_i w_j Cov(\sigma_i, \sigma_j)$$

  where σ_i are the uncertainties of the individual channels.

COMMENT: σ_i is the combination of statistical, systematic (different sources) and luminosity uncertainties. The different contribution are treated as fully correlated (background estimation, acceptance, luminosity ...) or uncorrelated (statistics, τ trigger ...).

RESULT:

$$\sigma(Z \to \tau\tau, m_{inv} = 66 - 116\ GeV) = 0.92 \pm 0.02(\text{stat}) \pm 0.08(\text{syst}) \pm 0.03(\text{lumi})\text{nb}$$

with $\chi^2/\text{ndof} = 1.24/2$.